Acta Materialia 193 (2020) 202–209

Contents lists available at ScienceDirect

Acta Materialia

journal homepage: www.elsevier.com/locate/actamat

Full length article

A unified kinetic model for stress relaxation and recovery during and after growth interruptions in polycrystalline thin films

Piyush Jagtap*, Eric Chason

School of Engineering, Brown University, Providence, Rhode Island, 02912, USA

ARTICLE INFO

Article History:
Received 15 December 2019
Revised 31 March 2020
Accepted 8 April 2020
Available online 3 May 2020

Keywords:
Polycrystalline thin films
Residual stress
Kinetic model
Growth interuuption
Grain boundary

ABSTRACT

A model for the kinetics of residual stress evolution is described that can be applied to both the relaxation during a growth interruption and the recovery following resumption of growth. The stress is attributed to simple atomistic processes based on reversible diffusion of atoms in and out of the grain boundary. Each of these processes is considered separately to understand how the rates differ during relaxation and recovery and how they depend on grain size, film thickness, temperature, deposition rate, and initial stress. The model is compared with experimental data obtained by others for several materials (Fe, Ni and Au).

1. Introduction

Polycrystalline thin films are used in innumerable technological applications. The residual stress that develops during the deposition process can often limit their performance [1,2]. Understanding the atomistic mechanisms leading to the generation of stress and their dependence on growth conditions is of paramount importance to predict and control these stresses. In this regard, the stress evolution during the thin film growth and the growth interrupts have been extensively studied recently [3–15]. Much of our knowledge on the origin of stress in thin films is based on *in-situ* stress measurement techniques such as laser-optics based wafer curvature measurement or cantilever deflection measurement. The resulting curvature is dependent on the product of the thickness-averaged film stress and the film thickness (referred to as the stress-thickness or force per width (F/w)). Real time wafer curvature measurements while the film is growing have provided valuable insights into the underlying atomistic processes occurring during thin film growth.

Many metallic polycrystalline thin films show Volmer-Weber growth mode wherein initially individual islands are nucleated on the substrate which later coalesce together forming a continuous layer. Further essentially uniform growth occurs during continued deposition. Abermann and Koch [16, 17] showed that atoms with low mobility (Type I) develop tensile stress during deposition and the stress remains constant during the growth interruption. In Type II materials with inherently higher mobility, stress changes from tensile to compressive stress with thickness and a significant amount of stress is relaxed when the growth is interrupted [16, 17].

Several mechanisms have been proposed to explain the stress evolution during different stages of thin film growth [17–19]. For instance, development of tensile stress during the stage of film coalescence is attributed to the layers in adjacent grains “zipping” together to form a grain boundary [20, 21]. The development of compressive stress in the post-coalescence stage for type II materials is still controversial [7, 22,23], but one proposed mechanism is diffusion of atoms from the surface into the grain boundary driven by the non-equilibrium surface conditions during deposition [3]. These processes are proposed to occur simultaneously during deposition in the vicinity of a grain boundary. Therefore, grain boundaries play an important role in the stress generation and relaxation processes when deposition flux is turned on and off [8, 24,25].

Other insights into stress have been provided by extensive studies focusing on the reversible stress evolution behavior observed during the growth interruptions of films with high atomic mobility (Type II) [7–15]. A few notable experimental observations commonly observed during a growth interrupt are (i) The initial compressive stress changes in the tensile direction upon the interruption of growth and the relaxed stress is almost completely recovered when the growth is resumed [7–15] (ii) the kinetics of stress relaxation during a growth interruption and stress recovery during growth resumption may be different [9,11,13,14] (iii) The kinetics of relaxation and recovery depend on the film thickness, grain size, temperature, deposition rate and initial value of stress [9–15]. Furthermore, it has been shown that during long interruptions a part of the relaxed stress is non-reversible and therefore it may be associated with other

* Corresponding author.
E-mail address: piyush_jagtap@brown.edu (P. Jagtap).

https://doi.org/10.1016/j.actamat.2020.04.013
1359-6454/

processes occurring in the bulk such as grain growth and recrystallization [12].

To address these issues, we have developed a kinetic model for stress relaxation and recovery during growth interruption and resumption. The model considers simplified mechanisms that focus on the stress generated at the grain boundaries by the processes such as coalescence and adatom insertion in the boundary during growth. The atoms can also diffuse out of the grain boundary when the growth is interrupted. The kinetic models are compared with experimental data from others in which the necessary parameters are monitored or controlled. We demonstrate that this model captures the kinetics of both relaxation and recovery of stress during interruption and resumption and also predicts its complex dependence on multiple parameters such as grain size, film thickness, deposition temperature, deposition rate, and initial stress.

2. Description of model

The model used in this work is similar to one we have previously described for post-coalescence stress during the growth of polycrystalline thin films [3, 26]. It is based on stress-generating mechanisms that are proposed to occur in the grain boundaries, where the broken crystal symmetry makes it easier to accommodate a change in the number of atoms in the film and hence generate strain. In this previous work, the difference in the rates of diffusion into and out of the grain boundary was described in terms of the difference in chemical potential of atoms in the two regions. Although this is formally correct, it is difficult to interpret because the actual chemical potentials are not known. In the current work, these rates are described more explicitly. As discussed below, there are separate terms for the rates of atoms going into the grain boundary, $(dN_{gb}/dt)_{in}$, and coming out of the grain boundary $(dN_{gb}/dt)_{out}$. This enables us to separately consider the processes of stress relaxation (when the film growth is interrupted) and stress recovery (when the film growth is resumed). Note that tables summarizing the key equations of the model, the parameters in them and their physical meaning are provided in the supplemental material

The model includes two opposing stress-generating mechanisms that create tensile and compressive stress. Tensile stress is described using the mechanism proposed by Hoffman [20,21]. When two islands coalesce to form a grain boundary, they become strained by an amount σ_T as long as the resulting strain energy is less than the reduction in interfacial free energy. Compressive stress is attributed to the subsequent insertion of atoms into the grain boundary [3]. The resulting average stress in the layer is then given by

$$\sigma = \sigma_T - \frac{M_f a^3}{L\, h_{gb}\, w} N_{gb} \tag{1}$$

In this expression, N_{gb} is the total number of atoms inserted into the grain boundary after it has formed. w is the film width, L is the grain size, h_{gb} is the film thickness, a^3 is the nominal volume of an atom and M_f is the biaxial modulus of the film. Note that this expression for the stress assumes that diffusion is fast in the grain boundary so that stress is uniform throughout the thickness of the layer. This is consistent with previous work on modeling the stress evolution in thin layers of Ni during film growth [27] and is appropriate for the other relatively thin layers considered in this work. This assumption may not be correct for thicker films or lower mobility systems. Other models have also been described in which the inserted atoms are confined to the top of the grain boundary [28] but they will not lead to the analytical expressions derived in this work.

Differentiating the above equation allows the rate of change of stress in the film $(\frac{d\sigma}{dt})$ to be related to the rates of atoms going into and out of the grain boundary $(\frac{dN_{gb}}{dt})$ and of forming new segments of grain boundary $(\frac{dh_{gb}}{dt})$:

$$\frac{d\sigma}{dt} = \frac{-M_f a^3}{L\, h_{gb} w}\left[\left(\frac{dN_{gb}}{dt}\right) - N_{gb}\frac{\frac{dh_{gb}}{dt}}{h_{gb}}\right] \tag{2}$$

We assume that the grain boundary height changes at roughly the same rate as the film thickness so that $(\frac{dh_{gb}}{dt})$ is approximately equal to the growth rate R. The changing number of atoms in the grain boundary can be broken into two parts

$$\left(\frac{dN_{gb}}{dt}\right) = \left(\frac{dN_{gb}}{dt}\right)_{in} - \left(\frac{dN_{gb}}{dt}\right)_{out} \tag{3}$$

where $(dN_{gb}/dt)_{in}$ is the rate at which atoms are inserted into the grain boundary from the surface and $(dN_{gb}/dt)_{out}$ is the rate at which atoms diffuse out of the grain boundary.

The driving force for these transitions is the chemical potential of atoms in each region which is assumed to be affected by the growth flux and stress conditions. During film growth, the chemical potential of atoms on the surface is elevated due to the arrival of new atoms from the vapor (by an amount defined as $\delta\mu_s$). If the film has stress, the chemical potential of atoms in the grain boundary is changed by $-\sigma a^3$. This scenario is shown schematically in Fig. 1. Even in the absence of growth flux or stress, the chemical potentials on the surface and grain boundary are not necessarily the same.

For atoms jumping from the surface into the grain boundary, the rate can be described by

$$\left(\frac{dN_{gb}}{dt}\right)_{in} = \left(\frac{2w}{a}\right)\left(\frac{dN_{gb}}{dt}\right)_{in,0} e^{\frac{+\delta\mu_s}{kT}} \tag{4}$$

where $(\frac{dN_{gb}}{dt})_{in,0}$is the rate of atoms jumping into the grain boundary per edge site when the growth rate is turned off, i.e., the surface concentration is equal to the equilibrium value. $(2w/a)$ is the number of surface sites that are adjacent to the grain boundary. During deposition, the elevation of the surface chemical potential by $\delta\mu_s$ increases the rate of atoms jumping into the grain boundary by a factor $e^{\frac{+\delta\mu_s}{kT}}$.

The nominal rate per site without supersaturation, $(\frac{dN_{gb}}{dt})_{in,0}$, can be related to more fundamental kinetic processes by writing it as

$$\left(\frac{dN_{gb}}{dt}\right)_{in,0} = X_{in}\frac{2}{a^2} D_{0,in}\, e^{\frac{E_{in}}{kT}} \tag{5}$$

where X_{in} is the dimensionless fraction of mobile adatoms on the surface adjacent to the grain boundary and $\frac{2}{a^2} D_{0,in}\, e^{\frac{E_{in}}{kT}}$ is the rate of transitions of these adatoms per site.

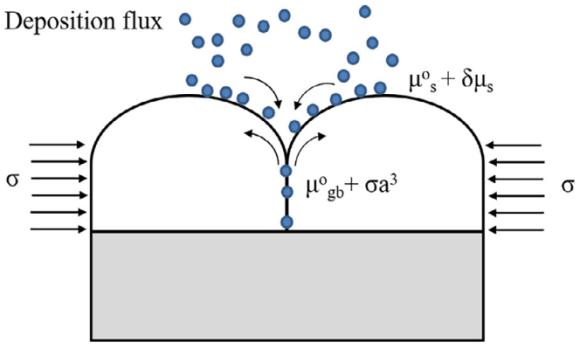

Fig. 1. Schematic illustration of a growth process during the film deposition. The chemical potential of atoms on the surface and grain boundary in equilibrium state are $\mu^o{}_s$ and $\mu^o{}_{gb}$, respectively. The deposition flux and presence of stress enhances the chemical potentials from their equilibrium value. The difference between the chemical potential of atoms on the surface and grain boundary lead to reversible diffusion of atoms in and out of a grain boundary.

For atoms jumping from the grain boundary onto the surface:

$$\left(\frac{dN_{gb}}{dt}\right)_{out} = \left(\frac{w}{a}\right)\left(\frac{dN_{gb}}{dt}\right)_{out,0} e^{\frac{\sigma a^3}{kT}} \tag{6}$$

where $(\frac{dN_{gb}}{dt})_{out,0}$is the rate of atoms jumping from the grain boundary onto the surface per site when the average stress in the film is equal to zero. When there is stress in the film, the jumping rate out of the boundary is modified by the factor $e^{\frac{\sigma a^3}{kT}}$. Note that, a tensile stress (positive σ) decreases the rate of atoms leaving the grain boundary and a compressive stress enhances the rate.

The rate per site without stress, $(\frac{dN_{gb}}{dt})_{out,0}$, can be related to more fundamental kinetic processes by

$$\left(\frac{dN_{gb}}{dt}\right)_{out,0} = X_{gb}\frac{2}{a^2}D_{0,gb}\, e^{\frac{E_{gb}}{kT}} \tag{7}$$

where X_{gb} is the dimensionless fraction of sites at the top of the grain boundary from which an atom can make a transition to the surface, and $\frac{2}{a^2}D_{0,gb}\, e^{\frac{E_{gb}}{kT}}$ is the rate of transitions for an atom to jump out of the grain boundary when there is no stress.

The ratio between the unenhanced rates into and out of the grain boundary can be defined in terms of a difference in chemical potential ($\Delta\mu_o$) between atoms on the surface ($\mu^o{}_s$) and in the grain boundary ($\mu^o{}_{gb}$):

$$\frac{\left(\frac{dN_{gb}}{dt}\right)_{out,0}}{2\left(\frac{dN_{gb}}{dt}\right)_{in,0}} = e^{\frac{\Delta\mu_0}{kT}} \tag{8}$$

where, $\Delta\mu_o = \mu^o{}_s - \mu^o{}_{gb}$. The factor of 2 in the denominator accounts for the fact that atoms can jump into the grain boundary from two different sides. Putting this into the stress evolution equation, we obtain

$$\frac{d\sigma}{dt} = \frac{-2M_f a^2}{L\, h_{gb}}\left(\frac{dN_{gb}}{dt}\right)_{in,0}\left[e^{\frac{\delta\mu_s}{kT}} - e^{\frac{\left(\sigma a^3 + \Delta\mu_0\right)}{kT}}\right] + (\sigma_T - \sigma)\frac{\frac{dh_{gb}}{dt}}{h_{gb}} \tag{9}$$

During growth, the competition among these rates leads to a steady-state (i.e., when $d\sigma/dt=0$) that depends on the growth conditions and material parameters, assuming that the grain size is not changing significantly during the growth.

For small deviations from equilibrium, the term $e^{\frac{\delta\mu_s}{kT}} - e^{\frac{(\sigma a^3 + \Delta\mu_0)}{kT}}$ can be replaced by $\frac{\delta\mu_s + \sigma a^3 + \Delta\mu_0}{kT} = \frac{\Delta\mu}{kT}$. This predicts a steady-state stress that is given by

$$\sigma_{ss} = \frac{\sigma_T + \sigma_C\left(\frac{\beta D}{RL}\right)}{\left(1 + \left(\frac{\beta D}{RL}\right)\right)} \tag{10}$$

where $\sigma_C = \frac{-(\delta\mu_s + \Delta\mu_0)}{a^3}$ and $\beta D = \frac{4M_f a^3}{kT} X_{in} D_{0,in}\, e^{\frac{E_{in}}{kT}}$. The effects of grain growth on the stress are not included in the model described here, but can be added (see Ref. [27]).

3. Kinetic model for stress relaxation during growth interrupt

This section applies the above analysis to describe the kinetics of stress relaxation during an interruption in the growth. When the deposition flux is stopped, $\frac{dh_{gb}}{dt}$ is equal to zero and the last term in Eq. (9) can be neglected. In addition, the higher chemical potential of adatoms on the surface due to supersaturation is no longer maintained and $\delta\mu_s$ = 0. Under these conditions, the relaxation kinetics are described by:

$$\frac{d\sigma}{dt} = \frac{-2M_f a^2}{L\, h_{gb}}\left(\frac{dN_{gb}}{dt}\right)_{in,0}\left[1 - e^{\frac{\left(\sigma a^3 + \Delta\mu_0\right)}{kT}}\right] \tag{11}$$

This is a first order differential equation that can be solved to obtain:

$$\sigma = \sigma_f + \frac{kT}{a^3}\ln\left(1 - \left(1 - e^{\frac{\left(\sigma_0 - \sigma_f\right)a^3}{kT}}\right)e^{\frac{-\beta D t}{L\, h_{gb}}}\right) \tag{12}$$

σ_o is the stress when the relaxation starts at time $t=0$. The relaxation kinetics do not depend explicitly on the pre-interruption growth conditions, but they influence it indirectly through the dependence on the initial stress (σ_o) when the growth is interrupted.

σ_f is the final value that the stress will relax to at very long times. In some previous work, the long-term stress was assumed to be zero, but this is not necessarily true if the rates of transitions for atoms into and out of the grain boundary are not equal. When the ratio of these rates is $e^{\frac{\Delta\mu_0}{kT}}$ (Eq. (8)) then the final stress is given by $\sigma_f = \frac{-\Delta\mu_0}{a^3}$.

The effect of $\Delta\mu_o$ is difficult to determine from measurements of stress during growth since it cannot be separated from $\delta\mu_s$ in the steady-state stress in Eq. (10). For this reason, it was not considered in some prior analyses of growth experiments [19]. However, its effect can be seen more directly in relaxation experiments and needs to be included. If $\Delta\mu_0 < 0$, the rate of atoms coming out of the grain boundary is higher than the rate going in when there is no growth-induced supersaturation or stress in the film. This tends to make the film develop a tensile stress when there is no growth. The opposite happens if the sign of $\Delta\mu_o$ is reversed. As described in Section 5, experimental studies show that the final stress does relax to a non-zero value.

In past work [25] the stress was assumed to be small so that the exponentials terms could be linearized. In that case, the stress is predicted to decay exponentially as

$$\sigma = \sigma_f + (\sigma_0 - \sigma_f)e^{\frac{\beta D}{L\, h_{gb}}t} \tag{13}$$

The rate of relaxation predicted by this form is less than that described by Eq. (12).

4. Kinetic model for stress recovery during growth resumption

The same approach can be applied to explain the kinetics of stress recovery when the growth is resumed after an interrupt. Eq. (9) cannot be solved explicitly but an approximate form for the kinetics can be obtained by linearizing the exponential terms. Assuming that the grain boundary height increases at the same rate as the film thickness, then $\frac{dh_{gb}}{dt} \sim R$ and $h_{gb} = h_0 + Rt = R(t_0 + t)$ where h_0 is the thickness when the growth is interrupted at time t_0 and t is the time after the growth is resumed at $t=0$. The stress evolution is then given by

$$\frac{d\sigma}{dt} = \frac{-2M_f a^2}{L\, R(t_0 + t)}\left(\frac{dN_{gb}}{dt}\right)_{in,0}\frac{\delta\mu_s + \sigma a^3 + \Delta\mu_0}{kT} + (\sigma_T - \sigma)\frac{1}{t_0 + t} \tag{14}$$

Rearranging the terms, this becomes

$$\frac{d\sigma}{dt} = \frac{1}{t_0 + t}\left(\sigma_T - \frac{\beta D}{RL}\frac{\delta\mu_s + \Delta\mu_0}{a^3}\right) - \frac{\sigma}{t_0 + t}\left(\frac{\beta D}{RL} + 1\right) \tag{15}$$

The solution of this first order linear differential equation has the form

$$\sigma = \sigma_{ss} + \frac{\sigma_0 - \sigma_{ss}}{\left(\frac{h}{h_0}\right)^A} \tag{16}$$

where the power A is equal to $(1 + \frac{\beta D}{RL})$ and h is the total film thickness. σ_o and h_o are the stress and thickness when the growth is resumed at $t=0$ and σ_{SS} is the steady-state stress during growth at rate R. This solution assumes that the grain size is constant, but the grain size dependence of σ_T and the time dependence of L could be included in the solution of Eq. (14) if the grain size changes significantly during the recovery.

5. Comparison of kinetic models with experimental data

To determine its validity, the model described above is compared with some previously published experimental studies for Fe [7], Ni [29] and Au [12, 29]. The data for the analysis was obtained by digitizing the results in the papers which may lead to some error, but does not affect the overall conclusions. Additional details of the experimental conditions used in these works can be found in the individual manuscripts.

The parameters used to calculate the stress evolution from the model are presented in Tables 1–3 and discussed further below. Some of the parameters are related to the experimental conditions (temperature, thickness). The grain size parameters in the tables were either reported with the stress measurements [7] or estimated from the reported dependence on thickness [12, 30]. Other parameters were determined by using non-linear least squares fitting to minimize the difference between the data and the model, using Eq. (12) for relaxation and Eq. (16) for recovery. Because the model is not exact, the difference between the data and fit cannot be attributed solely to experimental error and we cannot use statistical analysis to determine the error bars on the obtained parameters. Based on fitting results, the parameter for the nominal atomic size a was chosen to have a single value for each material; 0.43 nm was used for Fe and 0.63 nm for Ni. These values are two to three time larger than the values expected from the actual density.

The other fitting parameters were allowed to vary independently for each set of data. Since the parameter σ_0 is only used to set the initial value of the stress when the measurement is started, it does not depend on the kinetics of relaxation or recovery. Therefore, for each set of measurements there are only two fitting parameters that depend on the kinetics: σ_f and βD for relaxation and σ_{ss} and A for recovery. Ideally the parameters σ_{ss}, βD and A should be essentially constant for each set of processing conditions. Indeed, we find that the variation in the σ_{ss} parameter is small (~ 5%) when the growth is resumed at the same growth rate. However, for βD and A there is more variation in the fitting values obtained. For example, the value of βD for Ni is derived from the relaxation measurements in the final column of Table 2; the average and standard deviation is 7.1 +/- 4.8, 5.9 +/- 3.7 and 4.0 +/- 1.1 nm^2/s for temperatures of 398, 423 and 473, respectively. Similarly, the average and standard deviation for the parameter A is 38 +/- 27, 23 +/- 11 and 55 +/- 10 for temperatures of 398, 423 and 473, respectively. This error is in the range of 30 - 40 % which is significant. However, it is not clear whether this is due to uncertainty in the fitting procedure or to problems with the model. The physical meaning of these parameters and their trends with thickness and growth conditions are considered further in the discussion section.

Koch et al. [7] measured stress relaxation and recovery in Fe films during growth interruption, including its dependence on grain size and thickness. The results for the stress-thickness (F/w) vs. time are shown as the symbols in Fig. 2. The results from fitting the data to the model are shown as the solid lines. The parameters obtained from fitting two intervals of relaxation (starting at thicknesses of 20 and 35 nm) are shown in Table 1a (along with the grain size and thickness at the start of the relaxation and recovery). The value of σ_0 is determined by the starting conditions. The value of the final stress, σ_f, is found to be positive (tensile) for both relaxation intervals. The time constant for relaxation $(\frac{\beta D}{L}\ h)^{-1}$ is 6200 s for the first interrupt and 1700 s for the second interrupt. When the parameter βD is extracted from the relaxation time, it has an average value of 0.20 +/- 0.23 nm^2/s. The parameters from fitting the recovery data to the power law behavior predicted in Eq. (16) are shown in Table 1b. The exponent from fitting the data (defined as A in Eq. (16)) has a value of 10.7.

Yu and Thompson measured relaxation and recovery in Ni and Au at several different temperatures [12, 29]. They determined that there are two different time scales of relaxation and fit their results to the sum of two exponentials. The slow process, which has a relaxation time that is two orders of magnitude larger than the fast process, is the dominant process in the relaxation kinetics presented in Ref. [12]. Yu and Thompson attribute this to the effect of grain growth in the film. We believe that their analysis is correct, so therefore the slow relaxation and grain growth are not considered in this paper. Instead, we focus on the relaxation kinetics during shorter interrupts that can be found in Ref. [29]. This corresponds to the reversible fast process described in [12] and is appropriate for comparison with the model.

Measurements of relaxation and recovery in Ni are shown as the symbols in Fig. 3 for different temperatures indicated in the figure. The data corresponds to periods of growth at a rate of 0.04 nm/s followed by interruptions for relaxation and then recovery during resumption of growth. The data presented starts with the first growth interruption of 300 s after 36 nm of growth. This is followed by two more sequences of 10 nm of growth followed by 300 s interruptions at thicknesses of 46 and 56 nm. The results from fitting to our models are shown as the solid lines with the corresponding parameters in Table 2 for (a) relaxation and (b) recovery.

For each temperature, there are three sets of relaxation, identified by their starting thicknesses of 36, 46 and 56 nm. The fitting suggests that the final stress, σ_f, is more compressive at higher growth temperatures. The time constant for relaxation is on the order of hundreds of seconds which is consistent with the results for fast relaxation reported by Yu and Thompson [12]. The relaxation rate $(\frac{\beta D}{L}\ h)$ does not appear to depend strongly on the film thickness or the temperature. This is in agreement with the results reported by Yu and Thompson, but it does not agree with the dependence predicted by the model. However, we note that only a small range of h and L is covered in the experiments.

The recovery data corresponds to two periods of 10 nm growth. The steady-state stress is similar for each period at the same temperature. The steady-state stress is more compressive at higher temperatures, which is consistent with other measurements [30]. The value of the exponent varies from 19 to 62 with an average value of 38.7 +/- 20.2.

Yu and Thompson also studied relaxation and recovery in Au [12]. In this work, they present measurements for the recovery of

Table 1
Parameters used in calculation of (a) relaxation and (b) recovery for Fe shown in Fig. 2. The grain sizes in the table were reported with the stress measurements [7]. The relaxation parameters (σ_0, σ_f and ßD) and the recovery parameters (σ_0, σ_{ss} and A) were obtained from the fitting procedure.

a) Temperature T(K)	Thickness h_{gb} (nm)	Grain size L (nm)	σ_0 (Gpa)	σ_f (Gpa)	ßD/Lh (1/s)	ßD (nm^2/s)
520	20	10.4	-0.087	0.438	0.000161	0.0334
520	35	17.2	-0.288	0.054	0.000605	0.364

b) Temperature T (K)	h_0 (nm)	average grain size (nm)	σ_0 (GPa)	σ_{ss} (GPa)	A
520	20	13.8	0.184	-0.272	10.65

Table 2
Parameters used in calculation of (a) relaxation and (b) recovery for Ni shown in Fig. 3. The grain sizes in the table were estimated from measurements [29]. The relaxation parameters (σ_0, σ_f and ßD) and the recovery parameters (σ_0, σ_{ss} and A) were obtained from the fitting procedure.

a) Temperature T (K)	Thickness h_{gb}(nm)	Grain size L (nm)	σ_0 (GPa)	σ_f (GPa)	ßD/Lh (1/s)	ßD (nm^2/s)
398	36	12.857	0.001	0.073	0.0034	1.606
398	46	16.428	-0.032	0.025	0.0123	9.366
398	56	20	-0.027	0.031	0.0091	10.268
423	36	12.857	-0.076	-0.009	0.0044	2.076
423	46	16.428	-0.111	-0.049	0.0081	6.155
423	56	20	-0.117	-0.053	0.0084	9.475
473	36	12.857	-0.282	-0.220	0.0059	2.755
473	46	16.428	-0.300	-0.229	0.0064	4.901
473	56	20	-0.283	-0.198	0.0039	4.457

b) Temperature T (K)	h_0 (nm)	average grain size (nm)	σ_0 (GPa)	σ_{ss} (GPa)	A
398	36	14.642	0.047	-0.029	18.94
398	46	18.214	0.013	-0.032	57.2
423	36	14.642	-0.031	-0.108	14.64
423	46	18.214	-0.053	-0.113	30.48
473	36	14.642	-0.233	-0.301	48.34
473	46	18.214	-0.241	-0.280	62.39

Table 3
Parameters used in calculation of recovery for Au shown in Fig. 4. The grain sizes in the table were estimated from measurements [12]. The recovery parameters (σ_0, σ_{ss} and A) were obtained from the fitting procedure.

Temperature T (K)	h_0 (nm)	average grain size (nm)	σ_0 (GPa)	σ_{ss} (GPa)	A
300	44	18.571	-0.076	-0.139	25.514
300	60	24.107	-0.087	-0.132	30.643
300	75	29.464	-0.091	-0.125	37.879

the Au stress after interrupts of 5 min at 300 K and 0.05 nm/s. However, the data for the stress relaxation is not shown at the early stages so it was not possible to analyze it in terms of the fast relaxation process. Therefore, we only analyze the recovery kinetics here.

The measurements of stress recovery after resumption of growth at thicknesses of 44, 60 and 75 nm are shown in Fig. 4. The fit to the model is shown as the solid lines and the fit parameters are in Table 3. Fitting the data to the power law model, the average value of the exponent is 31.3 +/- 6.2. The steady-state stress becomes slightly less

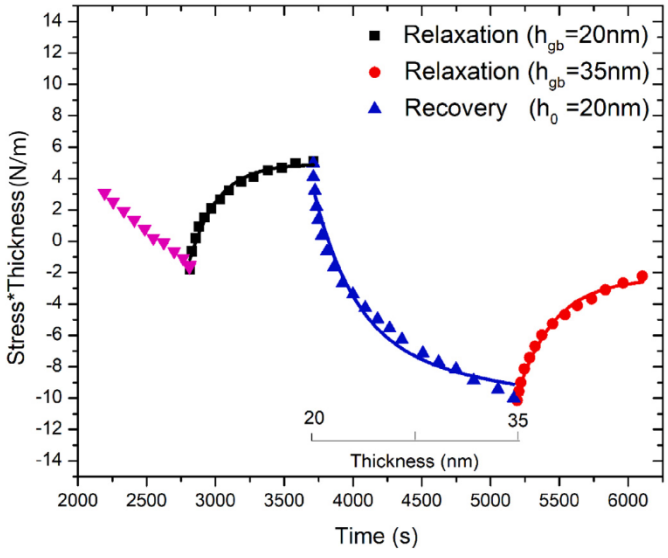

Fig. 2. Stress relaxation and recovery of Fe films deposited at 520K during growth interruption. The data was digitized from Ref. [7]. The solid lines represent fits to the model for relaxation and recovery. The fitting parameters are listed in the corresponding tables.

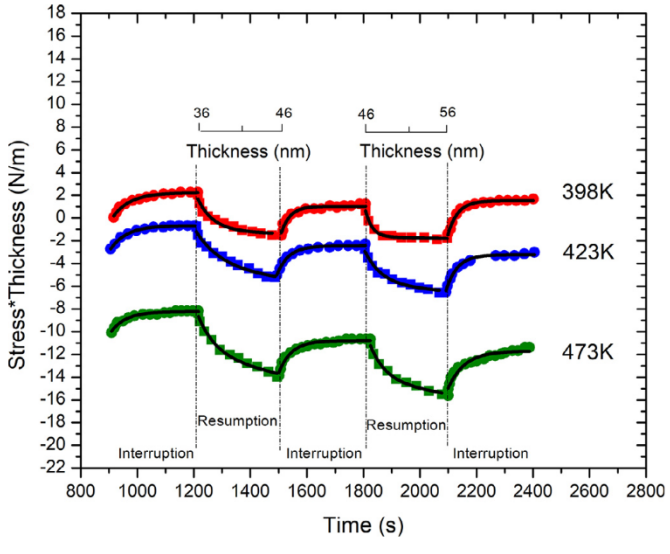

Fig. 3. Stress relaxation and recovery in Ni films deposited to different thicknesses at temperatures from 398–473K indicated in figure. The data was digitized from Ref. [29]. The solid black lines represent fits to the model for relaxation and recovery. The fitting parameters are listed in the corresponding tables. The periods of interruption and resumption are shown using vertical dashed lines.

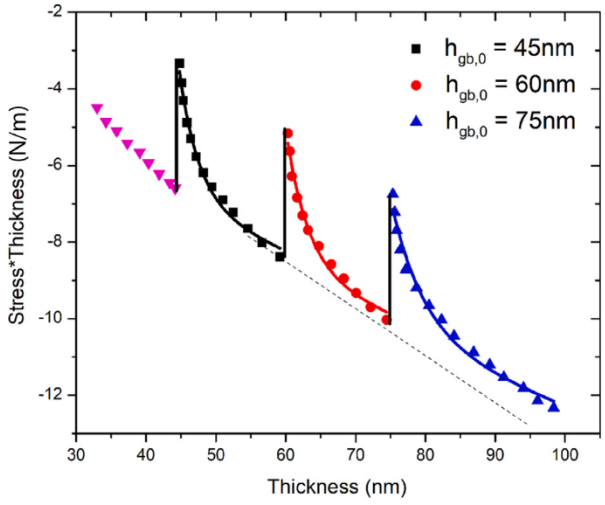

Fig. 4. Stress recovery during resumption in growth of Au films at 300 K after 5 min interruptions at thicknesses indicated by vertical lines. The data was digitized from Ref. [12]. The solid colored lines represent fits to the model for recovery with the fitting parameters listed in the corresponding tables. The dashed line represents the stress-thickness extrapolated from the steady state value before the second interrupt.

compressive for the larger film thickness which may be due to an increase in the grain size with thickness.

6. Discussion

In the following discussion, we consider some of the implications of the results obtained from this analysis as well as some shortcomings and potential sources of error. The model assumes that diffusion is fast enough so that the stress in the grain boundary is essentially uniform, which enables analytical expressions to be derived for the stress evolution. It is worth considering the basis for this assumption. In previous work, a high grain boundary mobility model was found to be consistent with quantitative analysis of stress-thickness evolution during deposition of Ni films [27] up to 200 nm thick. This would no longer be valid if the film is too thick, but the thicknesses of all the films discussed in the current work were less than 100 nm. In addition, measurements of the grain boundary diffusivity suggest the assumption is appropriate. For example, measurements in Ni at 400 K find that the grain boundary diffusivity is on the order of 3×10^{-18} m^2/s [31]. The corresponding diffusion distance during the observed relaxation time of 120 s is $\sim$ 20 nm which is similar to the thickness of the films (36 – 56 nm). Furthermore, the fact that the model is able to fit data for several material systems provides additional support for using the mechanisms contained in it. Therefore, using the high mobility model is not unreasonable. If the grain boundary diffusion were not high enough, the stress evolution would still be qualitatively similar to that predicted by the model. However, there would be gradients in the stress through the thickness of the film and the kinetics would not fit the equations described here. It is possible to consider this regime with numerical solutions, but that has not been done in this work.

A good feature of the model is that the form for the relaxation in Eq. (12) fits the data better than the simple exponential form (Eq. (13)) that has been proposed previously. This suggests that it is necessary to consider the exponential dependence of the transition rate on the film stress. The model also suggests a connection between the relaxation and the recovery kinetics where the exponent for recovery, A, depends on the relaxation parameters βD. For comparison, the average value of $(1+\frac{\beta D}{RL})$ calculated using the results obtained from the relaxation measurements in Fe is 2.39, The exponent determined from fitting the power law relaxation is 10.65. For the Ni relaxation, the average values of $(1+\frac{\beta D}{RL})$ are 11.8, 10.0 and 7.1 for the temperatures of 398, 423 and 473, respectively. The corresponding values obtained from fitting the recovery data are 38, 23 and 55. Hence the values of A obtained from the recovery experiments are typically higher than the values predicted from the relaxation experiments. Part of this disagreement may be due to the fact that the equation for the recovery kinetics was obtained by linearizing the exponential terms in the stress evolution equation even though they are outside of the linear regime. Although the agreement is not exact, it is generally consistent with the trend that larger values of $\frac{\beta D}{RL}$ correspond to a larger exponent for the recovery rate.

It is also useful to consider whether the values obtained from the fitting are reasonable by comparing with other experiments. To do this, we examine the values of βD obtained from fitting the Ni relaxation at 398 K which have an average value of 7.1 nm^2/s. The meaning of βD in terms of different physical constants is given in the description of Eq. (10) which relates it to the product of $X_{in}D_{in}$. This can further be related to the product $X_{gb}D_{gb}$ by applying Eq. (8). Using the fitting value of σ_f= 0.43 GPa to determine $\Delta\mu_0$ and a value of 290 GPa for the biaxial modulus of Ni, this suggests that $X_{gb}D_{gb}$ is equal to 1.9×10^{-21} m^2/s. Note that D_{gb} is proportional to the rate of transitions out of the grain boundary and is not the same as the grain boundary diffusivity. However, if we use the value of the grain boundary diffusivity (3×10^{-18} m^2/s) as an estimate of D_{gb}, then we obtain a value for the fraction of mobile atoms in the grain boundary (X_{gb}) to be 1.2×10^{-5}. This is probably an underestimate of D_{gb} which suggests that the number of mobile sites in the grain boundary might be higher.

The parameter σ_{ss} describes the steady-state stress that the film reaches during continuous growth. It depends on the growth conditions, but as shown in the tables, it returns to nearly the same value (within 5%) after each growth resumption for Ni (Table 2) and Au (Table 3). Other measurements of the steady-state stress at different growth conditions indicates that it becomes more compressive when the temperature is increased [29]. The values of the fitting parameters in Tables 2 are consistent with this trend for the steady-state stress at different temperatures.

The equations developed here assume that the contribution of grain growth is small, so it is important to consider the relative magnitude of the stress induced by grain growth. As described by Yu and Thompson, in the absence of grain growth the stress evolution after short interrupts should be reversible, i.e., the stress-thickness should return to essentially the same behavior as if the interrupt had not been performed. This can be estimated by extrapolating the behavior before the interrupt to larger thickness and comparing with the measured stress-thickness after the interrupt. This is shown by the dashed line in Fig. 4. The stress-thickness evolution after the interrupt returns to within 1.5 N/m of the value it would have developed based on the extrapolation of the measured behavior, a difference of only 12%. The small contribution of grain growth is also consistent with estimates of the grain growth kinetics in Fe from the reported grain sizes [7]. The grain size is estimated to change from 10.4 to 10.6 nm during the 15 min interrupt at 520 K, assuming kinetics of the form $d^2 = d_0^2 + kt$ [12]. Using the approach described by Yu and Thompson [30], this would change the stress-thickness by 0.9 N/m which is also relatively small compared to the measured change of 7 N/m during the relaxation.

The model predicts the dependence of the kinetic parameters on variables such as the thickness and growth rate which can be compared with the experimental results. The time scale for the relaxation in the model depends on $\frac{\beta D}{L}\ h_{gb}$, but the fitting parameters do not appear to depend strongly on the thickness in the analysis of Ni relaxation. Similarly, the values of βD obtained for Ni relaxation at different temperatures decrease at higher temperatures, whereas they would be expected to increase at higher temperatures if the diffusivity has Arrhenius behavior. Part of the disagreement may be due to the imperfect digitization of the data which contributes uncertainty

to the resulting parameters, but this is difficult to estimate. We also note that the parameters were obtained by fitting each set of data independently. The expected dependence of the parameters on thickness and temperature was not put into the fitting form. However, if we force the parameters to have the expected model dependence, we can still obtain reasonable fits (these results are not shown). Therefore, we attribute the difference between the parameters' dependence on grain size and temperature to the uncertainty in determining these parameters. More data over a wider range of thicknesses and temperatures would be useful for determining their effect on the kinetic parameters more precisely.

Alternatively, the weak dependence of the relaxation rate on the film thickness may point to a deviation between the experiments and the assumptions used to derive the model. It was assumed that the mobility in the grain boundaries is high and the stress is uniform throughout the thickness of the film. However, as discussed above, if the atomic mobility is not sufficiently high, relaxation may not occur uniformly throughout the film thickness. It may occur instead primarily by diffusion of atoms out of the grain boundary closer to the surface. In that case the relaxation rate would not depend as strongly on the thickness of the film as predicted by our model. For comparison, previous measurements of stress relaxation in Sn films [25] which have high atomic mobility do show the predicted dependence on the film thickness.

The parameter σ_f is an estimate of the final stress that the film reaches after a long period of relaxation. As shown by the fitting parameters, it appears to depend on the film thickness. For instance, it is considerably more tensile after the first interrupt in Fe than after the second. As discussed above, this may indicate that the atoms do not diffuse out of the entire length of the grain boundary. If the film only relaxes near the surface, the final stress-thickness may be due to residual stress left unrelaxed in the bottom part of the film.

However, there may be a more fundamental reason for the observed behavior of σ_f. As described in the description of relaxation kinetics (Section 3), σ_f is a measure of the difference between the chemical potential of atoms on the surface and in the grain boundary ($\Delta\mu_0$). As the film grows, the grain shape and hence the ratio of surface to grain boundary area changes. Dependence of the chemical potential on the grain shape is seen in other phenomena such as zero-creep experiments [32–34]. In these studies, a metal in the form of a thin wire or foil has a tendency to decrease its length in order to achieve a shape of the grains that is closer to equilibrium. This occurs by atoms diffusing out of the grain boundary onto the surface of the grains. The process can be stopped by applying a stress to the wire (zero creep condition). The magnitude of the required stress depends on the deviation of the aspect ratio from the equilibrium value as well as the surface/interfacial energies [35]. This type of measurement has been used to determine the surface energy of materials [33–35]. The process behind this is similar to the diffusive mechanism contained in the stress model described here. It would suggest that in grains with an aspect ratio of free surface to grain boundary area (proportional to L/h_{gb}) that is larger than the equilibrium value, atoms would flow out of the grain boundary onto the surface to decrease L and increase h_{gb}. Since the film is attached to the substrate, this results in a tensile stress. In the early stages of film growth when grain boundaries are just beginning to form, the ratio of free surface to grain boundary height is likely to be large, which is consistent with the observed tensile stress at the early stages of film growth. As the film grows, the aspect ratio decreases which would make the stress less tensile/more compressive. Unlike stress induced by grain growth, the transition from steady-state stress during growth (σ_{SS}) to the final stress after relaxation (σ_f) is reversible. This is consistent with the behavior shown in Fig. 4 for repeated sequences of growth and interrupts. Although the effect of non-equilibrium grain shape is consistent with the measurements, it is not conclusive. Further measurements of both relaxation kinetics and grain size would be useful for determining the significance of this mechanism on stress evolution.

The analysis here is based on reversible diffusion into and out of the grain boundary, but we recognize that other mechanisms have been proposed that are not contained in our model. Because reversible changes occurring during growth interruptions have been observed both in pre-coalescence and post coalescence regime [9,36], it has been suggested that they are associated with reversible changes in defect concentrations on the surface such as density of steps, kinks, and adatoms [9,18,36]. However, the absence of reversible stress changes in epitaxial thin films suggest that grain boundaries play a crucial role during the relaxation and recovery process [8]. It has also been suggested that surface morphology changes such as grain boundary grooving play a role [13,14,29,37].

In addition, crucial parameters such as the grain boundary diffusivity may change with time. For instance, the grain boundary structure that develops during film deposition is likely to be highly defected. During long interruptions, it may evolve toward a more dense structure that would have lower mobility and prevent the stress from changing in it. In this case, the assumption of high grain boundary mobility may not remain valid over time.

It should be emphasized that the work described here does not rule out other possible mechanisms playing a role in stress evolution. Based on the studies considered here, it appears that the model can account for a wide range of measurements, but it does not mean that other mechanisms are not possible or might be dominant under different conditions.

7. Conclusion

A model for the kinetics of stress relaxation and recovery has been developed. It considers that the driving forces for diffusion of atoms in and out of a grain boundary are fundamentally different. The rate of atoms diffusing into the grain boundary is affected by the supersaturation of atoms on the surface whereas the flux of atoms jumping out of the grain boundary depends exponentially on the stress. This produces an observed asymmetry between the relaxation and recovery processes.

The significance of the model presented is that it provides a quantitative estimate of both the relaxation and recovery kinetics that can be compared directly with experiments and used to extract kinetic parameters. The model is shown to agree with experimental results in Fe, Ni and Au and used to obtain kinetic parameters. It is hoped that the model will be applied to other systems in order to develop a coherent picture of the processes controlling residual stress in thin films.

Declaration of competing interest

The authors declare that they have no known competing financial interests or personal relationships that could have appeared to influence the work reported in this paper.

Acknowledgment

This work was supported by the National Science Foundation (NSF) under Contract No. DMR-1602491. Enlightening discussions with Frans Spaepen are greatly appreciated.

Supplementary materials

Supplementary material associated with this article can be found in the online version at doi:10.1016/j.actamat.2020.04.013.

References

[1] I. Mizushima, P.T. Tang, H.N. Hansen, M.A. Somers, Residual stress in Ni–W electrodeposits, Electrochim. Acta 51 (2006) 6128–6134.
[2] J. Matovic, Application of Ni electroplating techniques towards stress-free microelectromechanical system-based sensors and actuators, Proc. Inst. Mech. Eng. Part C J. Mech. Eng. Sci. 220 (2006) 1645–1654.
[3] E. Chason, B.W. Sheldon, L.B. Freund, J.A. Floro, S.J. Hearne, Origin of compressive residual stress in polycrystalline thin films, Phys. Rev. Lett. 88 (2002) 156103.
[4] J. Leib, C.V. Thompson, Weak temperature dependence of stress relaxation in as-deposited polycrystalline gold films, Phys. Rev. B 12 (2010) 121402.
[5] J.A. Floro, S.J. Hearne, J.A. Hunter, P. Kotula, E. Chason, S.C. Seel, C.V. Thompson, The dynamic competition between stress generation and relaxation mechanisms during coalescence of Volmer–Weber thin films, J. Appl. Phys. 89 (2001) 4886–4897.
[6] C. Friesen, S.C. Seel, C.V. Thompson, Reversible stress changes at all stages of Volmer–Weber film growth, J. Appl. Phys. 95 (2004) 1011–1020.
[7] R. Koch, D. Hu, A.K. Das, Compressive stress in polycrystalline Volmer-Weber films, Phys. Rev. Lett 94 (2005) 146101.
[8] J. Leib, R. Monig, C.V. Thompson, Direct evidence for effects of grain structure on reversible compressive deposition stresses in polycrystalline gold films, Phys. Rev. Lett. 102 (2009) 256101.
[9] C. Friesen, S.C. Seel, C.V. Thompson, Reversible stress changes at all stages of Volmer–Weber film growth, J. Appl. Phys. 95 (2004) 1011–1020.
[10] J.A. Floro, S.J. Hearne, J.A. Hunter, P. Kotula, E. Chason, S.C. Seel, C.V. Thompson, The dynamic competition between stress generation and relaxation mechanisms during coalescence of Volmer–Weber thin films, J. Appl. Phys. 89 (2001) 4886–4897.
[11] D.Z Flötotto, M. Wang, L.P. Jeurgens, E.J. Mittemeijer, Kinetics and magnitude of the reversible stress evolution during polycrystalline film growth interruptions, J. Appl.Phys. 118 (2015) 055305.
[12] H.Z. Yu, J.S. Leib, S.T. Boles, C.V. Thompson, Fast and slow stress evolution mechanisms during interruptions of Volmer-Weber growth, J. Appl. Phys. 115 (2014) 043521.
[13] Enrique Vasco, Celia Polop, Intrinsic compressive stress in polycrystalline films is localized at edges of the grain boundaries, Phys. Rev. Lett. 119 (2017) 256102.
[14] E. Vasco, E.G. Michel, C. Polop, Disclosing the origin of the postcoalescence compressive stress in polycrystalline films by nanoscale stress mapping, Phys. Rev. B 98 (2018) 195428.
[15] J. Leib, C.V. Thompson, Weak temperature dependence of stress relaxation in as-deposited polycrystalline gold films, Phys. Rev. B 82 (2010) 121402.
[16] R. Koch, The intrinsic stress of polycrystalline and epitaxial thin metal films, J. Phys. Condensed Matter 6 (1994) 9519.
[17] R. Abermann, Measurements of the intrinsic stress in thin metal films, Vacuum 41 (1990) 1279–1282.
[18] Frans Spaepen, Interfaces and stresses in thin films, Acta Materialia 48 (2000) 31–42.
[19] Eric Chason, Pradeep R, Guduru, Tutorial: Understanding residual stress in polycrystalline thin films through real-time measurements and physical models, J. Appl. Phy. 119 (2016) 191101.
[20] R.W. Hoffman, Stresses in thin films: The relevance of grain boundaries and impurities, Thin. Solid Films 34 (1976) 185–190.
[21] R.W. Hoffman, Stress distributions and thin film mechanical properties, Surface Interface Anal. 3 (1981) 62–66.
[22] C. Friesen, C.V. Thompson, Comment on “Compressive Stress in Polycrystalline Volmer-Weber Films”, Phys. Rev. Lett. 95 (2005) 229601.
[23] R. Koch, D. Hu, A.K. Das, Koch Hu, Das Reply, Phys. Rev. Lett. 95 (2005) 229602.
[24] G. Abadias, E. Chason, J. Keckes, M. Sebastiani, G.B. Thompson, E. Barthel, G.L. Doll, C.E. Murray, C.H. Stoessel, L. Martinu, Stress in thin films and coatings: Current status, challenges, and prospects, J. Vacuum Sci. Technol. A Vacuum Surfaces Films 36 (2018) 020801.
[25] J.W. Shin, E. Chason, Compressive stress generation in Sn thin films and the role of grain boundary diffusion, Phys. Rev. Lett. 103 (2009) 056102.
[26] Eric Chason, A kinetic analysis of residual stress evolution in polycrystalline thin films, Thin Solid Films 526 (2012) 1–14.
[27] E. Chason, A.M. Engwall, Z. Rao, T. Nishimura, Kinetic model for thin film stress including the effect of grain growth, J. Appl. Phys. 123 (2018) 185305.
[28] E. Chason, J.W. Shin, S.J. Hearne, L.B. Freund, Kinetic model for dependence of thin film stress on growth rate, temperature, and microstructure, J. Appl. Phys. 111 (2012) 083520.
[29] Hang Yu, Mechanism for intrinsic stress evolution during and after polycrystalline thin film growth, Ph.D thesis, Massachusetts Institute of Technology, 2013.
[30] H.Z. Yu, C.V. Thompson, Grain growth and complex stress evolution during Volmer–Weber growth of polycrystalline thin films, Acta Mater. 67 (2014) 189–198.
[31] B.S. Bokstein, H.D. Bröse, L.I. Trusov, T.P. Khvostantseva, Diffusion in nanocrystalline nickel, Nanostructured Mater. 6 (1995) 873–876.
[32] E.D. Hondros, Influence of phosphorus in dilute solid solution on the absolute surface and grain boundary energies iron, Proc. R. Soc. Lond. Ser. A-Math. Phys. Sci. (1965) 479 286 (1407).
[33] D. Josell, F. Spaepen, Determination of the interfacial tension by zero creep experiments on multilayers—I. Theory, Acta Metallurgica et Mater. 41 (1993) 3007–3015.
[34] D. Josell, F. Spaepen, Determination of the interfacial tension by zero creep experiments on multilayers—II. Experiment, Acta Metallurgica et Mater. 41 (1993) 3017–3027.
[35] Frans Spaepen, Chemical potentials driving diffusional flow in multilayers, Mater. Sci. Forum 154 (1994) 43–54.
[36] C. Friesen, C.V. Thompson, Reversible stress relaxation during precoalescence interruptions of Volmer-Weber thin film growth, Phys. Rev. Lett. 89 (2002) 126103.
[37] Hang Z. Yu, Carl V. Thompson, Correlation of shape changes of grain surfaces and reversible stress evolution during interruptions of polycrystalline film growth, Appl. Phys. Lett. 104 (2014) 141913.